

## Article

# A Study on the Effect of Particle Size on Li-Ion Battery Recycling via Flotation and Perspectives on Selective Flocculation

Tommi Rinne, Natalia Araya-Gómez  and Rodrigo Serna-Guerrero \* 

Department of Chemical and Metallurgical Engineering, School of Chemical Engineering, Aalto University, 02150 Espoo, Finland

\* Correspondence: rodrigo.serna@aalto.fi

**Abstract:** The recycling of active materials from Li-ion batteries (LIBs) via froth flotation has gained interest recently. To date, recycled graphite has not been pure enough for direct reuse in LIB manufacturing. The present work studied the effect of particle sizes on the grade of recycled graphite. Furthermore, selective flocculation is proposed as a novel approach to control particle sizes and thus improve graphite grade by preventing the entrainment of cathode components. Zeta potential and particle size measurements were performed to find an optimal pH for electrically selective flocculation and to study the interaction of flocculants, respectively. Batch flotation experiments were performed to investigate the effect of particle size on the purity of the recovered graphite. Results suggested that, in the absence of ultrafine fine particles, battery-grade graphite of 99.4% purity could be recovered. In the presence of ultrafine particles, a grade of 98.2% was observed. Flocculating the ultrafine feed increased the grade to 98.4%, although a drop in recovery was observed. By applying a dispersant in addition to a flocculant, the recovery could be increased while maintaining a 98.4% grade. Branched flocculants provided improved selectivity over linear flocculants. The results suggest that particle size needs to be controlled for battery-grade graphite to be recovered.

**Keywords:** lithium-ion batteries; direct recycling; froth flotation; selective flocculation



**Citation:** Rinne, T.; Araya-Gómez, N.; Serna-Guerrero, R. A Study on the Effect of Particle Size on Li-Ion Battery Recycling via Flotation and Perspectives on Selective Flocculation. *Batteries* **2023**, *9*, 68. <https://doi.org/10.3390/batteries9020068>

Academic Editors: Pascal Venet, Karim Zaghib and Seung-Wan Song

Received: 2 December 2022

Revised: 13 January 2023

Accepted: 16 January 2023

Published: 17 January 2023



**Copyright:** © 2023 by the authors. Licensee MDPI, Basel, Switzerland. This article is an open access article distributed under the terms and conditions of the Creative Commons Attribution (CC BY) license (<https://creativecommons.org/licenses/by/4.0/>).

## 1. Introduction

The extensive recycling of lithium-ion battery (LIB) components is nowadays considered essential as a result of the forecasted increase in the demand of raw materials for electrification. Although the composition of end-of-life LIB streams varies depending on their specific cathode chemistry, they typically contain potentially valuable materials such as Li, graphite, Co, Mn, Ni, Cu, and Al [1–3]. State-of-the-art recycling technologies have focused on recovering only those elements with high economic value, such as Co, Ni, and Cu, either via pyrometallurgical or hydrometallurgical processes [4,5]. Recently, the recycling of Li has started gaining traction, as a recycling rate of 70% was mandated by the EU in the 2020 Batteries Regulation proposal [6]. Graphite has also been listed as a critical raw material within the EU [7], and it is thus expected that its recycling will gain importance in the near future [8,9].

Direct recycling of LIBs is a novel approach that provides means for recovering all the electrode components of the battery, including Li and graphite. What makes direct recycling particularly appealing is that the electrode materials are recovered in a chemical form fit for purpose, since battery waste does not undergo further chemical processes. In general, direct recycling consists of two steps: (1) mechanically separating the battery components into individual material streams, and (2) restoring the original performance of the recovered materials [10]. The industrial implementation of direct recycling processes, however, is currently hindered by the difficulty of recovering concentrates with high purity, as grades of >99% would be required for optimal performance of the recycled electrodes. Due to the relatively low value of graphite, this high purity requirement makes its separation uneconomical, and it is often treated as an impurity in the recycling process.

During direct recycling processes, shredding, crushing, and sieving are usually applied to produce a stream containing the high-value electrode components, commonly referred to as “black mass.” Subsequently, the separation of anode and cathode should be performed by a physical separation operation, among which froth flotation has been considered as an interesting option by several authors [11–22]. Flotation is a unit operation that exploits differences in the wettability of materials. Its operating principle thus makes flotation suitable for black mass processing since it is typically accepted that graphite is naturally hydrophobic, while the Li-metal oxide cathodes have a hydrophilic character [10,23]. It is therefore expected that graphite particles will attach to bubbles and be selectively collected in the froth phase, while Li-metal oxides remain in suspension and are recovered in the underflow [24,25]. However, due to the factors discussed in the following paragraphs, the flotation process is not perfectly selective.

In the context of LIB black mass, the main factor limiting the selectivity of flotation is the imperfect liberation of the active particles. Consequently, most published research on black mass flotation has concentrated on the preprocessing stages required to increase the liberation degree of the particles, and especially to degrade the binder materials that hinder the separation [10]. However, it is hypothesized in the present article that flotation selectivity is also hindered by the ultrafine particle size of the cathode active materials via mechanical entrainment—a factor that has been neglected in most prior studies. The main aim of the present article is to evaluate the contribution of ultrafine cathode particle entrainment to the loss of selectivity in black mass flotation.

It has been shown that industrial black mass contains significant quantities of ultrafine particles, mostly from the cathode active material [17,18,26]. For example, a typical industrial NiMnCoO<sub>2</sub>/LiCoO<sub>2</sub> (NMC/LCO) black mass has been reported to have a d<sub>10</sub> of 2.7 μm, and a d<sub>50</sub> of 16.9 μm [18]. It is generally accepted that flotation performs optimally when separating particles between 15 μm and 150 μm in size [27]. Ultrafine particles of <10 μm, however, are more vulnerable to being mechanically entrained in the froth, due to fluid drag forces becoming dominant over the hydrophobic/hydrophilic interactions for particles of small mass [28,29]. In the context of black mass flotation, this phenomenon increases the non-selective recovery of hydrophilic cathode particles in the froth and lowers the grade of the graphite concentrate, even if the active particles are fully liberated. Thus, it is hypothesized that excess entrainment needs to be prevented to recover battery-grade graphite from black mass via froth flotation. In addition to evaluating the magnitude of the fine cathode particle entrainment, the present article makes the first reported effort of entrainment prevention via particle size control of the black mass.

Preventing entrainment can be achieved by increasing particle sizes prior to flotation by the selective formation of cathode agglomerates—a process known as selective flocculation [30]. A similar approach has been recently investigated by other researchers studying the fine particle flotation of natural minerals [28,31]. Furthermore, selective flocculation has been researched with regard to the separation of chromite tailings [32–34], feldspars minerals [35], low-grade iron ore fines such as hematite, kaolinite, and siderite [36–40], iron oxide, and silica suspensions [41]; coal flotation [42–44]; and the recovery of rare earths [45,46] and complex copper ores [47], to cite some examples. However, in the context of black mass flotation, this approach has not yet been explored, to the best of the authors’ knowledge.

In general, selective flocculation is a technique proposed to aggregate and separate solid-solid mixtures of ultrafine particle size [30]. In selective flocculation, particle agglomeration is induced by adding a polymeric material (flocculant) in a dispersed phase [30]. Flocculant agents can be synthetic or natural polymers [30,48]. The effectiveness of flocculants is determined by their molecular mass (or chain length), polymer backbone structure (branched/linear), ionic strength, pH, fluid mixing, the charge density of the molecule, and the dosage of the flocculant. Once flocs are formed, their separation can be performed via flotation, elutriation, or thickening, for example [30]. In the present article, flotation was chosen as the method of floc separation.

Selectivity in flocculation operations is influenced by particle characteristics (e.g., particle size, particle surface heterogeneity, and surface potential), the electrochemical environment of the suspension (e.g., pH and other dissolved species), the properties of the flocculant polymers (e.g., ionic character and molecular weight), and the mechanical parameters of mixing (e.g., agitation rate and the type of impeller) [48,49]. Selective flocculation can be achieved, for example, by altering the surface potential of particles, by controlling the contact time between particles, by selective polymer chemisorption, or by coating impurities [49]. Furthermore, Somasundaran and Runkana [49] proposed that the dispersion of the fines and flocculant adsorption are determined in selective flocculation. The probability of particles selectively aggregating depends on the interactions between similar particles. Floc formation can be achieved by “(1) a reduction in the electrostatic repulsion between particles; (2) formation of polymer bridges between particles; (3) ion-exchange reactions between polymers and particle surfaces” [49].

Considering all of this, the present study investigated an electrically selective flocculation process. Zeta potentials of analytically pure graphite and LCO were individually measured in a wide range of pH to identify a pH region in which a zeta potential gradient existed for the components. pH control was then utilized in an attempt to achieve electrically selective flocculant adsorption on the cathode particle surfaces. Four different flocculants of varying ionic strength and polymer backbone structure were studied, and sodium hexametaphosphate was tested as a selective graphite dispersant to prevent anode-cathode heteroflocculation.

In summary, the aim of the present study was to evaluate the contribution of cathode entrainment to the loss of purity in the graphite froth concentrate, by studying fully liberated model systems of analytically pure graphite and LCO with ideal and realistic particle sizes. Furthermore, particle size control via selective flocculation is suggested. Particle size distributions of model systems were presented by applying various flocculants/flocculant concentrations at a fixed pH. Flotation experiments were then performed to compare the purity of the recovered graphite concentrates in the flocculated and non-flocculated systems. Furthermore, this study presents a data interpretation methodology that can be utilized to evaluate the selectivity of flocculation in a two-component system, when flotation is applied as a method of floc separation.

## 2. Materials and Methods

### 2.1. Mineral Samples and Chemicals

#### 2.1.1. Minerals

Since this study marks the first exploratory work on the selective flocculation of black mass, analytically pure  $\text{LiCoO}_2$  (LCO) and graphite were used as mineral samples. The properties of the minerals, including the distributor, mineral composition, and purity, are listed in Table 1. Furthermore, Table 1 lists the abbreviations for each mineral used later in this paper to distinguish between individual mineral samples. In certain experiments, different LCOs and graphite were mixed with a 1:1 wt.-% ratio to obtain a “model black mass” mixture.

**Table 1.** Properties of the minerals used in the study.

Distributor	Mineral	Abbreviation	Purity [%]
Sigma-Aldrich, St. Louis, MO, USA	$\text{LiCoO}_2$	LCO-C	99.8
MSE Supplies, Tucson, AZ, USA	$\text{LiCoO}_2$	LCO-F	>99.5
ProGraphite GmbH, Untergriesbach, Germany	Spherodized graphite	Graphite	99.95

In Table 1, the abbreviations have been derived from the properties of the mineral samples. As will be shown in Section 3.2, LCO-C has a coarser particle size distribution compared to LCO-F.

### 2.1.2. Flocculants

Four different commercially available cationic polyacrylamide (CatPAM) flocculants were used in this study. The nominal properties of said flocculants (as provided by the distributor/manufacturer), are reported in Table 2. Furthermore, Table 2 lists the abbreviations used in this work for each flocculant.

**Table 2.** Properties of the flocculants used in the study.

Manufacturer	Trade Name	Ionicity	Molecular Weight	Polymer Backbone Structure	Abbreviation
Flinkenberg Chemicals Oy, Espoo, Finland	FinFloc PE445	Medium cationic	10 MDa	Linear	FF 445
SNF Floerger, Andrézieux, France	FO 4190 VHM	Low cationic	Very high	Linear	FO 4190
SNF Floerger Andrézieux, France	FO 4498 SSH	Medium cationic	N.A.	Branched	FO 4498
SNF Floerger Andrézieux, France	FO 5449 AF	Medium cationic	N.A.	Branched	FO 5449

Flocculant solutions were prepared by wetting a dry flocculant powder with ethanol at a 1:2 weight ratio and mixing vigorously by hand for 1 min. After this, ion-exchanged water was added to dissolve the flocculant at a target concentration of 0.5 wt.-%. Prior to usage, flocculant solutions were stirred for 24 h with a magnetic stirrer to ensure proper dissolution of the polymer. The 0.5 wt.-% mother solutions were further diluted to the target concentration before the experiments. Each individual mother solution was used within 48 h of preparation and discarded afterwards, in order to ensure that no significant degradation of the flocculant had occurred, as the age of the flocculant solution had been reported to influence the flocculant performance [50]. Throughout the lifetime of the flocculant solution, magnetic stirring was applied to ensure the stability of dissolution.

### 2.1.3. Flotation Reagents

HCl and NaOH (0.1 M, 99.5% purity) were applied as pH regulating agents. Methyl isobutyl carbinol (MIBC, 98% purity) was used as a frother in flotation experiments. Furthermore, sodium hexametaphosphate (SHMP, 96% purity) was tested as a dispersant in the flocculation/flotation experiments. All of the aforementioned chemicals were purchased from Sigma-Aldrich and were used without further purification.

## 2.2. Experimental Procedures

### 2.2.1. Zeta Potential Measurements

To determine the best potential pulp ionicity for electrically selective flocculant adsorption, the zeta potentials (ZPs) of LCO and graphite were measured as a function of pH. Measurements were carried out using a Malvern Panalytical Zeta sizer Nano ZS 90 (Malvern, United Kingdom). ZP values were measured in aqueous media within a pH range of 2–11. Aqueous solutions of HCl and NaOH totaling 0.1 M were used to adjust the pH, and the pH was measured using a Mettler Toledo SevenExcellence™ multi-channel pH meter (Greifensee, Switzerland). To ensure the stability of dispersions during the measurements, all studied samples were ground for 60 s in a ring mill (Fritsch Pulverisette 9, Idar-Oberstein, Germany) with a tungsten carbide grinding media. Ground samples were dispersed in the pH-adjusted water to form 0.01 wt.-% dispersions. Prior to each measurement, the dispersed samples were shaken vigorously for 30 s before pipetting them into a folded capillary cell (cell type DTS1070). Six measurements were carried out for each sample, and an average value was calculated. Based on the results of the ZP measurements, an optimal pH for selective flocculation was determined.

### 2.2.2. Particle Size Distribution Measurements

To study the interaction of the flocculants and the solid particles, particle size distributions (PSDs) of single and mixed mineral dispersions of LCO and graphite were measured in the presence of various flocculant concentrations, using a laser diffraction particle size analyzer (Malvern Panalytical Mastersizer 3000, Malvern, United Kingdom). PSD measurements were carried out in an aqueous medium at pH 5, as this was deemed the most suitable pH for selective flocculant adsorption based on the ZP measurements (as will be presented in Section 3.1). Under these conditions, the liquid medium had  $10^{-5}$  M ionic concentration of  $H^+$  and  $Cl^-$ .

Each PSD sample was prepared according to the following guidelines:

1. Dispersing a mineral sample into 25 mL of water that was pre-adjusted to pH 5 using HCl. Shaking vigorously by hand for 2 min to allow for proper mixing.
2. Pipetting the desired amount of dispersant (SHMP) into the dispersion, followed by 3 min of vigorous shaking by hand. Dispersant was only applied in mixed mineral measurements. In single mineral measurements, this conditioning step was not included.
3. Pipetting the desired amount of flocculant to the dispersion, followed by 3 min of vigorous shaking by hand to allow for floc formation and growth.
4. Adding the sample to 500 mL of pH 5-adjusted water, before starting the measurement immediately.

Five measurements were carried out for each sample, and an average distribution was calculated. Table 3 lists the parameters of the PSD measurements.

**Table 3.** Parameters in the particle size distribution measurements.

Mineral(s)	Flocculant Concentration [g/t]	Flocculant	Dispersant
LCO-C	0, 20, 50, 100, 150, 300	FF 445	None
LCO-F	0, 20, 35, 50, 100	FF 445, FO 4190, FO 4498, FO 5449	None
Graphite	0, 100	FF 445, FO 4190, FO 4498, FO 5449	None
LCO-C + G	0	None	None
LCO-F + G	0, 20, 35, 50, 100	FF 445, FO 4498	0.5 wt.-% SHMP

### 2.2.3. Flotation Experiments

Considering that the aim of the present work was the study of particle size in flotation, artificial black mass mixtures were produced to prevent unintentional influences caused by the contaminant species, particularly residual binders, present in industrially produced black mass.

Flotation experiments were performed using two different model black mass feeds, both of which had a distinctive particle size distribution. To analyze the influence of fine particles on flotation separation efficiency, and particularly on the grade of graphite, cathode materials with distinctive PSDs were selected. Firstly, an “ideal” black mass was prepared by mixing LCO-C and graphite, resulting in a mixture where active materials have similar particle size and where only ca. 14% are fine particles (herein defined as  $<10 \mu\text{m}$ ). Secondly, a “realistic” model black mass containing LCO-F and graphite was studied. As will be detailed in Section 3.2.2, the PSD of the “realistic” model black mass (ca. 27% of particles  $<10 \mu\text{m}$  in size) was expected to approach the properties of industrially obtained black mass, whose mechanical treatment typically results in fine cathode particles.

The separation efficiency achieved with the ideal model black mass was used as a benchmark, against which the realistic model black mass was compared (both with and without flocculants). It has been well-documented in the literature that particles can flocculate in mixed mineral systems, even if they resist flocculation as a single mineral system [30]. This phenomenon is known as heteroflocculation. The reason for heteroflocculation’s occurrence has been attributed to the entropic change in the flocculant polymer once it has adsorbed on its primary target mineral surface. The adsorption of the flocculant on the

target surface (e.g., LCO, as in the present study) alters the entropy of the polymer, possibly causing its subsequent adsorption on non-target surfaces to become thermodynamically stable [51]. For this reason, studying the selectivity of flocculation in mixed mineral systems is paramount for the development of a successful agglomeration process.

Two linear CatPAM flocculants (FF 445 and FO 4190), and two branched CatPAM flocculants (FO 4498 and FO 5449) were tested in this experimental series. Based on the results of the model black mass particle size measurements (Section 3.2.2), FO 4498 was deemed the best candidate for selective flocculant adsorption and was thus studied most thoroughly. Furthermore, sodium hexametaphosphate (SHMP) was applied as a dispersant due to its reported effectiveness in preventing the heterocoagulation of graphite and quartz [52]. The chemical parameters of all the conducted flotation experiments are shown in Table 4.

**Table 4.** The chemical parameters of the flotation experiments. Constant parameters, not listed in the table, include a pulp density of 40 g/L, an aeration rate of 2 L/min, and 8 ppm of MIBC (frother). The “ideal” model black mass was mixed using LCO-C and graphite, and the “realistic” was mixed using LCO-F and graphite.

Experiment	Model Black Mass	Flocculant/Concentration [g/t <sub>LCO</sub> ]	Dispersant/Concentration [g/t <sub>graphite</sub> ]
1	Ideal	None/“Pristine”	None
2	Realistic	None/“Pristine”	None
3	Realistic	FO 4498/10	None
4	Realistic	FO 4498/15	None
5	Realistic	FO 4498/20	None
6	Realistic	FO 4498/25	None
7	Realistic	FO 4498/35	None
8	Realistic	FF 445/15	None
9	Realistic	FO 4190/20	None
10	Realistic	FO 5449/20	None
11	Realistic	FF 445/15	SHMP/5000
12	Realistic	FO 4498/20	SHMP/5000

Batch flotation experiments were performed with a manually operated flotation device (Lab Cell—60 mm FloatForce mechanism, Outotec, Espoo, Finland) in a 1 L flotation cell. A total of 40 g of model black mass was first placed in the cell, followed by the addition of one liter of ion-exchanged water, preadjusted to pH 5 with HCl (measured with a Mettler Toledo SevenExcellence™ multi-channel pH meter), to obtain a solid-liquid ratio of 40 g/L. The pulp was then agitated with an impeller at 1000 RPM for 3 min to ensure proper mixing before adding surfactants. In the experiments where dispersants were used, the dispersant was added first, followed by 3 min of conditioning. After this, a flocculant was added, and the mixture was stirred for 3 min. Lastly, frother was added with a conditioning period of 2 min. Throughout mixing and conditioning, the impeller rate was kept at 1000 RPM. After this, the impeller rate was decreased to 850 RPM, and air was allowed to flow to the bottom of the cell via an outlet in the impeller at a flow rate of 2 L/min.

Once the airflow was initialized, the formation of froth started, marking the beginning of the experiment ( $t_{0 \text{ min}}$ ). Froth was first allowed to rise to a constant height, and froth collection started immediately after this. The first froth concentrate fraction was collected during the first minute of the experiment ( $t_{0-1 \text{ min}}$ ) by continuously scooping the froth into a container. The second froth concentrate was collected and placed in another container, by scooping 10 times/30 s during the timeframe  $t_{1-10 \text{ min}}$ . The third froth concentrate was collected by scooping 15 times/min for 15 min ( $t_{10-25 \text{ min}}$ ), or for as long as froth formation continued. The collected concentrates and underflow were then vacuum filtered and air dried in a convection oven at 40 °C for ca. 48 h. Figure 1 shows a schematic representation of the experimental procedure.

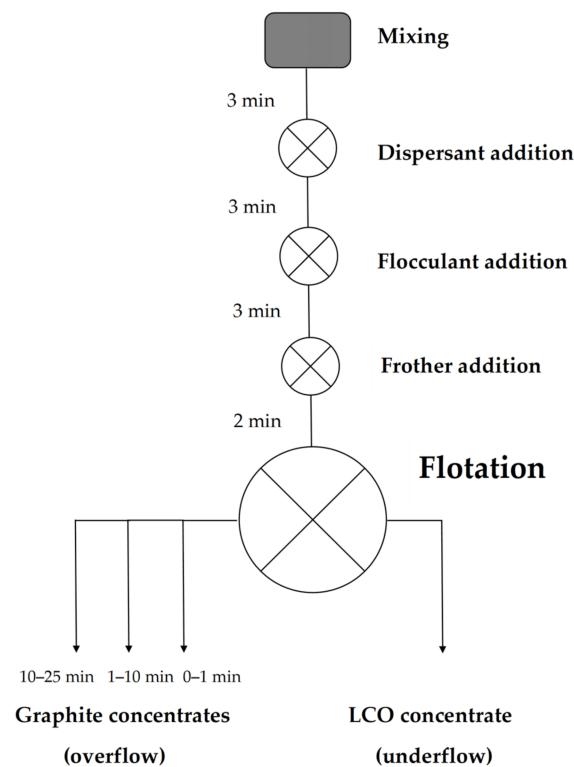


**Figure 1.** A schematic representation of the flotation experiments.

### 2.3. Characterization of Flotation Samples

After drying, the froth and underflow products were weighed and characterized for elemental compositions using a portable XRF gun (Oxford Instruments, X-MET 5000, Abingdon, United Kingdom). Five measurements spanning 30 s each were performed on each recovered sample, and an average value was calculated to account for the statistical variance of the composition on the sample surface. As the XRF gun can only analyze elements with atomic numbers  $\geq 20$ , Co was used as a marker element to determine the LCO grade of each sample. Since there were only two components in the model black mass, the LCO grades were easily transcribed to graphite grades by mass balance.

To improve the quantitative accuracy of the XRF analysis, a calibration curve was obtained from mixtures of LCO and graphite with known compositions. To generate the calibration curve, data points were gathered in 0.5 wt.-% intervals for the LCO grade range 0–5 wt.-%, and in 2.5 wt.-% intervals for the LCO grade range 5–20 wt.-%. The resulting curve was then used as a reference to adjust the measured XRF results.

The composition of the underflow was calculated via mass balance of the LCO content of the froth fractions and the known head grade of the flotation feed. In these calculations, the LCO/graphite head grades were adjusted based on the assumption that Li partially dissolves in the process water during flotation, as has been documented by other researchers [21]. The dissolution tendency of Li was measured by dispersing a model black mass sample in water (pH 5) under similar mechanical conditions as those applied in the flotation experiments and measuring the mass loss of the sample. The recorded mass loss equated to 45 wt.-% of Li dissolving in the process water during one flotation experiment, which coincides with the work of Salces et al. [21]. This equates to an adjusted black mass composition of 49.19 wt.-% cathode material (partially delithiated), and 50.81 wt.-% graphite after flotation.

### 3. Results

#### 3.1. Zeta Potential Measurements

Figure 2 shows the ZP values of graphite and LCO as a function of pH of the liquid medium. HCl and NaOH were used as pH regulating agents, resulting in the dominant ions in the pulp being  $H^+$  and  $Cl^-$  for the acidic pH range, and  $Na^+$  and  $OH^-$  for the basic pH range.

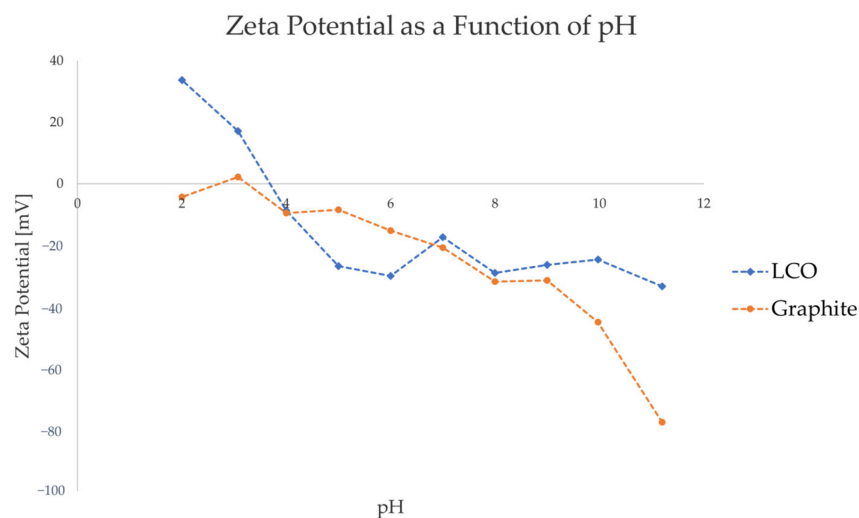


**Figure 2.** Zeta potential of graphite and LCO as a function of pH, with HCl and NaOH used as pH-regulating agents.

As seen in Figure 2, the ZP measurements indicate that, under the studied pulp conditions, the surface charge of graphite is approximately neutral or slightly negative in the pH range of 2–5, and increasingly negative in the pH range of 6–11. LCO, on the other hand, has a highly positive surface charge in the pH range of 2–3 and a highly negative surface charge in the range of 5–11, with the isoelectric point being between pH 3 and pH 4. Considering that neither LCO nor graphite contain chemically reactive functional groups, it is likely that the change in zeta potential at different pH levels results from the adsorption of ionic species of water. Indeed, Figure 2 reflects the generally accepted trend for inert surfaces and oxide minerals, with a positive charge in highly acidic conditions shifting to a negative charge in neutral and alkaline environments [53].

When identifying the candidate pH range for electrically selective flocculant adsorption on the LCO surface, a pH range of 2–3 would thus be favorable for anionic flocculants, and pH 4–11 for cationic flocculants. To avoid the flocculant from adsorbing on the graphite surface, the pH ranges 2–3 and 5–6 seem to be more suitable, as there is a significant difference in the surface charge of the two components in this region. To satisfy the general desire to minimize reagent consumption in a potential recycling process, pH 5 was chosen to be studied in the subsequent stages of this article. At this pH, a cationic flocculant is expected to be preferably adsorbed on the highly negative LCO surface, rather than on the graphite surfaces that have a comparatively weaker negative charge. This hypothesis was tested by performing particle size measurements of single active components and model black mass with varying types and concentration of flocculants.

#### 3.2. Particle Size Distribution Measurements

##### 3.2.1. Pure Active Components

PSDs were measured for pure LCO and graphite at pH 5 to study the effect of flocculant concentration on particle size. PSDs were first measured for non-flocculated samples, and flocculated samples were then compared against these baseline PSDs.

Figure 3 shows the frequency PSDs of the LCO samples as a function of flocculant concentration. Furthermore, cumulative PSDs are provided in Figure A1 in Appendix A.

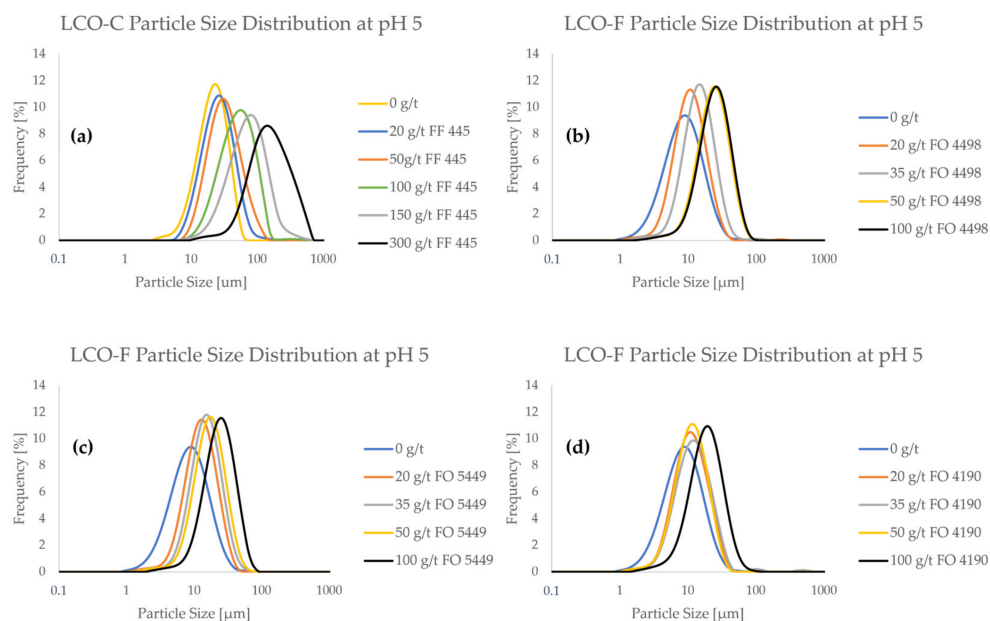


**Figure 3.** Particle size frequency distributions of LCO in the presence of flocculant at various concentrations at pH 5.

From Figure 3, it can be seen that both LCO samples interact with the CatPAM flocculants, as particle size consistently increased with higher flocculant concentration. Even a relatively small flocculant addition of 20 g/t influenced the particle size significantly. When looking at the PSDs of pristine (i.e., non-flocculated) LCO samples, it can be seen that LCO-C has significantly less ultrafine particles compared to LCO-F. Particle size measurements show that LCO-C contains ca. 10% of particles < 10  $\mu\text{m}$  (Figure A1a), whereas they represent up to 60% of LCO-F (Figure A1b–d). The difference in the fine particle content of the two samples is expected to significantly influence the separation efficiency of the material in flotation, as LCO-F particles are more prone to entrainment in the froth phase. Depending on the type of flocculant, a dosage of between 50 and 100 g/ton would be needed to approximate the particle size of pristine LCO-C.

A special interest is drawn to the effect of flocculant on ultrafine particle content. At 100 g/t of FF 445, the ultrafine particle content of LCO-C decreased to 0.5% (Figure A1a). For LCO-F, the use of 100 g/t of FO 4498, FO 5449, or FO 4190 reduced the <10  $\mu\text{m}$  particle fraction to 6.5% (Figure A1b), 7% (Figure A1c), and 15% (Figure A1d), respectively. Even if the ultrafine particles are difficult to eliminate altogether, their presence is affected even at low flocculant concentrations. When using only 20 g/t solutions of FO 4498 (Figure A1b), FO 5449 (Figure A1c), and FO 4190 (Figure A1d), the <5  $\mu\text{m}$  content of LCO-F was reduced from ca. 21% to 9%, 5%, and 9%, respectively.

Regarding the effect of flocculants on graphite, Figure 4 compares the PSDs of pristine particles and of those in the presence of 100 g/t for all the studied flocculants.

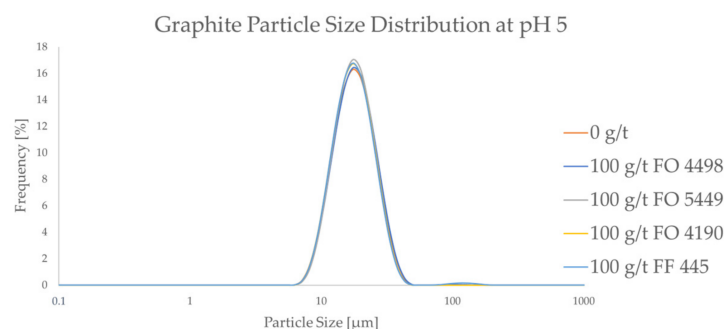


**Figure 4.** The particle size frequency distributions of graphite both without a flocculant and with a high dosage of a flocculant.

As seen in Figure 4, the PSD of graphite does not seem to be affected by the CatPAM flocculants, even at the relatively high dosage of 100 g/t. This trend is seen across all the studied flocculants. The results confirm that the studied CatPAM flocculants do not adsorb on graphite surfaces at pH 5. It can also be seen that the ultrafine particle content of the graphite is lower compared to the LCO samples. The  $d_{10}$  and the  $d_{50}$  values of the graphite sample were ca. 12  $\mu\text{m}$ , and 17  $\mu\text{m}$ , respectively. This suggests that the flocculant species chosen in this study can potentially be used to form selective agglomerates from the LCO-graphite mixture.

### 3.2.2. Model Black Mass

To study the flocculation phenomenon in model black mass, PSD measurements were carried out on 50:50 mixtures of LCO-F and graphite, in the presence of different flocculant molecules at various concentrations. Furthermore, reference PSDs were measured for non-flocculated model black mass samples of LCO-F + graphite and LCO-C + graphite. The reference PSDs are presented in Figure 5.

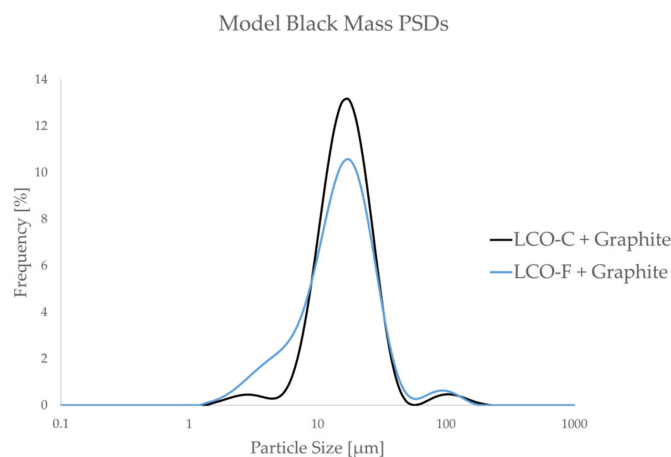


**Figure 5.** Particle size frequency distributions of model black mass samples in the absence of a flocculant at pH 5.

As Figure 5 shows, the model black mass composed of LCO-C and graphite contains significantly less ultrafine particles compared to that containing LCO-F. This is expected to result in a more efficient graphite separation in the LCO-C + graphite system, as the entrainment of ultrafine particles is avoided [28,31]. Thus, LCO-C + graphite is viewed as an “ideal” system, against which the separation efficiency of the “realistic” system (LCO-F + graphite) is compared to.

Figure 6 shows the frequency distributions of LCO-F + graphite mixtures as a function of flocculant concentration at pH 5. For these measurements, SHMP is added as a dispersant for the graphite at a fixed concentration of 5000 g/t<sub>graphite</sub>.

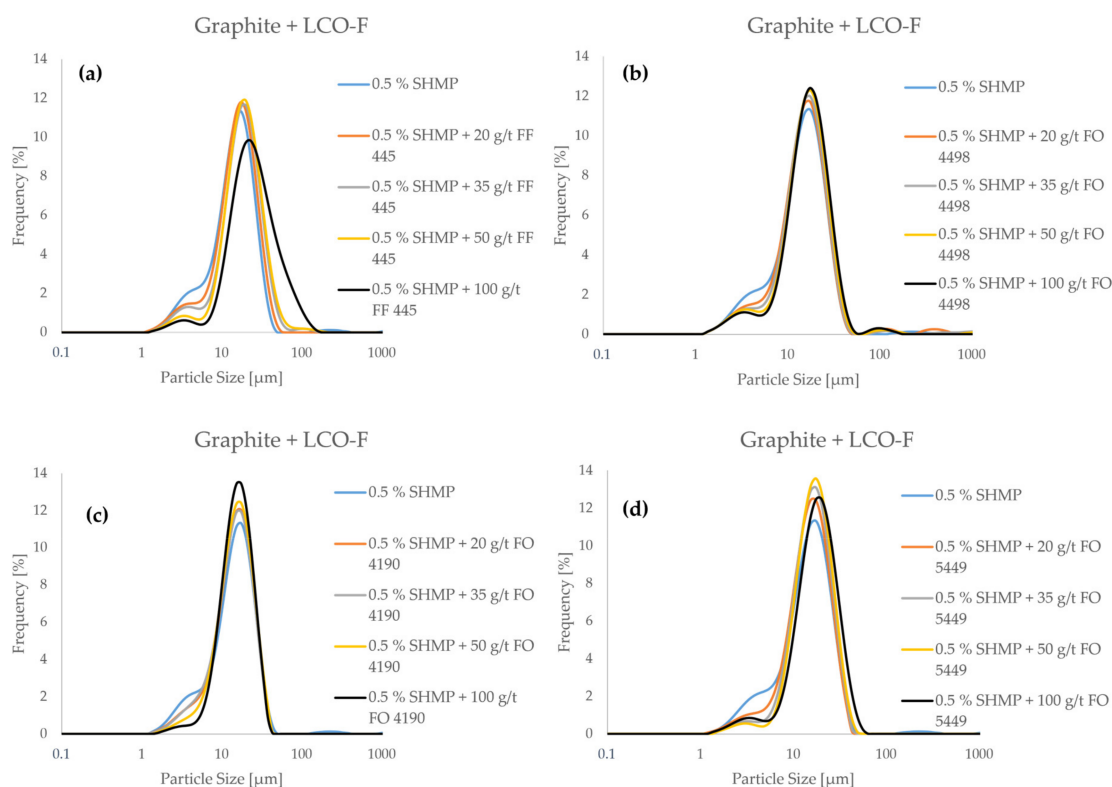


**Figure 6.** The particle size frequency distributions of a model black mass composed of LCO-F and graphite as a function of flocculant concentration in pH 5 (SHMP is applied as a dispersant).

From Figure 6, it can be seen that all four flocculants reduce the ultrafine particle content of the model black mass when applied alongside the SHMP dispersant. However, the characteristics of the PSDs were quite distinctive. FF 445 (Figure 6a) resulted in the most aggressive particle size growth, as the fine particle “shoulder” of the distribution is drastically reduced, and the whole distribution is shifted towards the coarse end of the spectrum. This means that the coarse particles in the system are also agglomerating when FF 445 is applied, an effect that may promote heteroflocculation. Similar behavior was observed in the case of FO 5449, when applying a concentration of 100 g/t (Figure 6d). In the case of FO 4498 (Figure 6b) and FO 4190 (Figure 6c), the agglomeration appears more subtle. With these flocculants, the fine particle count is reduced significantly, while the coarse particle count remains relatively stable. This might indicate better flocculation selectivity, as finer flocs are less likely to include graphite particles. However, in order to gain conclusive evidence on the selectivity of flocculation with the different flocculants, the characterization of flotation products is necessary.

### 3.3. Flotation Experiments

The grade-recovery curves (GRCs) of graphite are presented in Figure 7. As a general rule when reading GRCs, values towards the upper right corner represent a higher separation efficiency. The GRCs that have two data points indicate experiments that only lasted for 10 min, whereas three data points indicate experiments in which a third froth concentrate (10–25 min) was also collected. Data points from experiments in which a flocculant was successfully used to achieve a higher grade compared to the pristine black mass are highlighted with a dashed line.

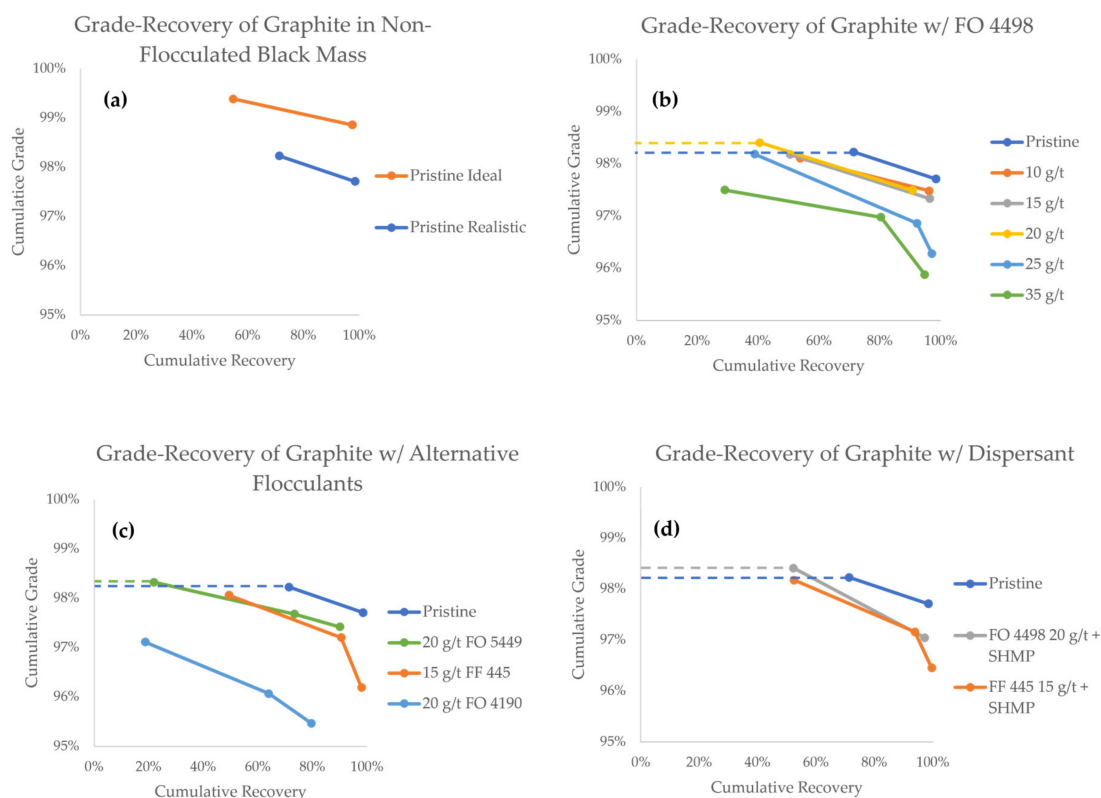


**Figure 7.** Grade-recovery curves for graphite in all flotation experiments.

The first comparison can be made between the pristine black mass samples, in which the particle size of LCO was the only variable (Figure 7a). In these experiments, the first minute concentrates show grades of 99.4% and 98.2%, with recoveries of 54.7% and 71.3%, for the ideal and realistic model black masses, respectively. The total cumulative graphite recoveries after 10 min were 97.6% and 98.4% for the ideal and realistic black masses, respectively, associated with grades of 98.9% and 97.7%, respectively. The difference in the graphite grade corroborates the notion that the particle size of LCO plays a vital role in its separation efficiency and entrainment tendency. It is therefore interesting to explore strategies to control the particle size of cathode materials in order to make direct recycling a feasible alternative.

Admittedly, the values of grade and recovery from the graphite product may appear remarkable, particularly compared with the work reported by other authors [12,13,18,21,54,55]. It should therefore be kept in mind that these experiments were performed on a model black mass, without the interference of residual contaminant species. Indeed, these results show that graphite with product quality purity (i.e.,  $\geq 99\%$ ) was obtained from the ideal black mass, where a lower recovery was acceptable. This is nevertheless an indication that direct recycling of LIB graphite via froth flotation is possible, provided that active particles are fully liberated, and that the PSD of the cathode material is optimized.

When looking at GRC results achieved with the FO 4498 flocculant (Figure 7b), a decrease in the overall graphite recovery is observed, as the flocculant concentration is increased. This is an undesired effect that could be reasonably explained by the formation of predominantly hydrophilic heteroflocs, in which graphite particles are trapped. During the first minute of the experiment, however, the graphite grade stayed virtually unaffected in the flocculant concentration range of 10–15 g/t, and at 20 g/t, the grade was slightly increased at 98.4%. It appears that within this concentration range, even if hydrophobic heteroflocs are formed, the flotation of unaffected graphite remains favored in the early stages of separation. From a process engineering perspective, the hydrophobic heteroflocs are kinetically outcompeted by the unaffected graphite particles.

Flocculant concentrations of 25 g/t and 35 g/t, however, consistently reported lower graphite grades, indicating that hydrophobic heteroflocs emerge in larger quantities at this concentration range. Unfortunately, even at the optimal 20 g/t FO 4498 concentration, the cumulative grade at the end of the experiment was lower than the grade achieved with pristine realistic feed. Under the conditions used in this study, the influence of slower floating hydrophobic heteroflocs became predominant by the end of the experiment.

Figure 7c shows a comparison between various flocculant species. When compared to FO 4498, 20 g/t FO 5449 results in a similar overall graphite recovery, but the kinetics of separation are hindered. The best grade reported in the 0–1 min concentrate fraction was achieved with FO 5449, which reported a value of 98.3%, compared with 98.2% in the pristine experiment. Considering that both FO 5449 and FO 4498 are branched polymers, we suggest that this type of flocculant is better suited for selective agglomeration. At a concentration of 20 g/t, the branched flocculants seemed to produce heteroflocs that were hydrophilic enough for the unaffected graphite to kinetically outcompete them for extraction in the froth. However, the recovery obtained with FO 5449 (i.e., 21.8%) was clearly lower than that with FO 4498 (i.e., 40.5%). This may be a consequence of the stronger cationic character of the former, which may result in stronger hydrophilic heteroflocs, preventing the flotation of graphite.

Contrary to branched flocculants, the two tested linear flocculants did not seem to offer a benefit under the conditions studied (Figure 7c). The decreasing grade and a virtually unaffected recovery suggests that, at 15 g/t, FF 445 predominantly produces hydrophobic heteroflocs, carrying both graphite particles and LCO to the froth phase. FO 4190 was the worst performing flocculant overall, producing lower kinetics, recovery, and grade. This may be a result of low agglomeration selectivity, producing both hydrophilic and hydrophobic heteroflocs.

With the aim of improving the selectivity of flocculation, experiments with FF 445 and FO 4498 were carried out using SHMP as a graphite dispersant. As seen in Figure 7d, the best result of this campaign was achieved when the dispersant was used in combination with FO 4498. For the first minute concentrate, a 98.4% grade was maintained while recovery was increased to 52.2%. In the case of FF 445, the dispersant can again be seen to have a positive effect on the kinetics, recovery, and grade of graphite, when compared against the experiment where no dispersant was used. With the SHMP dispersant, the final values of recovery and grade were 99.6% and 96.5%, respectively. The dispersant seems to work as expected, increasing the amount of unaffected graphite particles in the pulp, which are kinetically favored for their extraction in the froth phase. This suggests that, even in the presence of a dispersant, the properties of a flocculant impact the formation and hydrophobicity of the heteroflocs significantly.

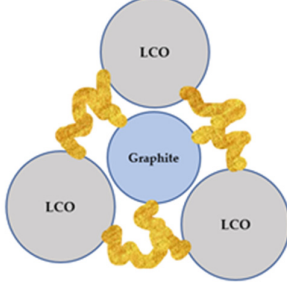
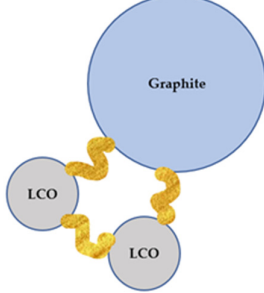
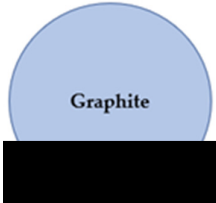
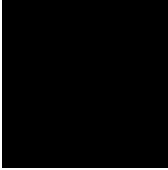
Based on the experimental data provided in the present study, branched flocculants seem to offer better selectivity compared to linear flocculants. Fundamental understanding of this improved selectivity would require data on the exact chemical structure of the functional groups in the studied flocculants, which unfortunately is not available from the data sheet provided by the suppliers. Potential mechanisms for improved flocculation selectivity, reported by other researchers, include stereoselectivity via steric hindrance, and chemisorption of certain flocculants on the target mineral surface [56]. Additional work is necessary to understand the mechanism of flocculation selectivity in LIB anode-cathode mixtures, and to find optimal conditions in which heteroflocculation is successfully prevented.

It must be stated that the grade of the recovered graphite remained extremely high (>95%) for every flocculant/concentration studied. Additionally, >90% recoveries were observed in all but one experiment (Figure 7c, FO 4190, with a recovery of 79.6%). This indicates that, under the studied flocculant concentrations, most of the graphite particles do indeed remain unaffected by the flocculant, even in the absence of a dispersant, and are readily recoverable in the froth. In order to increase the grade of the graphite concentrate, the formation of heteroflocs with a highly hydrophobic character needs to be carefully avoided. In view of this, branched CatPAM flocculants seem to provide the best starting point for further research.

#### 4. Discussions

Since flotation was chosen as a method of separation for the flocculated black mass, the grade-recovery data can be interpreted to gain information on the selectivity of the flocculation process. After a model black mass is treated with a flocculant, five types of particles potentially exist in the pulp: (i) hydrophilic selective LCO flocs; (ii) heteroflocs that are predominantly hydrophilic; (iii) preeminently hydrophobic heteroflocs; (iv) unaffected graphite particles; and (v) unaffected LCO particles. A schematic representation of each particle is presented in Table 5. Furthermore, Table 5 lists the wettability status of each particle type, and their anticipated behavior in a flotation system.

**Table 5.** The types of particles that can exist in the pulp after a flocculant has been added. The yellow ribbons schematically represent the flocculant polymers.

Schematic Representation of Particle	Type of Particle	Wettability	Separation Tendency	Mechanism of Extraction in Froth
	Selective LCO floc	Hydrophilic	Predominantly extracted in the underflow	Entrainment, dependent on particle size
	Heterofloc, high LCO content	Hydrophilic	Predominantly extracted in the underflow	Entrainment, dependent on particle size
	Heterofloc, low LCO content	Hydrophobic	Predominantly extracted in the froth phase	True flotation of graphite, entrapment of LCO
	Graphite, unaffected	Hydrophobic	Predominantly extracted in the froth phase	True flotation, kinetically favored over heteroflocs
	LCO, unaffected	Hydrophilic	Predominantly extracted in the underflow	Entrainment, dependent on particle size

The relative amount of each type of particle or agglomerate presented in Table 5 is likely influenced by the pulp chemistry, as the type/concentration of flocculant and the presence of a dispersant affect the heteroflocculation tendency of the solids [51]. This will result in a distinctive flotation behavior of the flocculated systems, when compared to the non-flocculated black mass. Furthermore, the difference in the degree of hydrophobicity of the heteroflocs in comparison with the unaffected graphite particles is likely to influence the separation kinetics.

When comparing the grade-recovery results of the flocculated system against the pristine system, the results reveal the following scenarios:

- If the recovery of graphite remains unaffected, but the grade is increasing, the system has successfully produced hydrophilic selective LCO flocs, which result in less entrained LCO.
- If the recovery of graphite remains unaffected, but the grade is decreasing, the system entails hydrophobic heteroflocs that are responsible for the true flotation of some of the LCO particles—a behavior that is akin to entrapment in the flotation of natural ores. This may counteract the benefit of less entrained LCO, even if the system is also producing hydrophilic LCO flocs.
- If the recovery of graphite is decreasing, hydrophilic heteroflocs have likely been produced, resulting in some of the graphite particles being non-recoverable in the froth.
  - a. If a decreasing graphite recovery is associated with a decreasing graphite grade, the system is expected to produce a mixture of hydrophilic and hydrophobic heteroflocs, and the hydrophobic heteroflocs will be responsible for true flotation of some of the LCO particles, counteracting the benefit of less entrained LCO.
  - b. If a decreasing graphite recovery is associated with an increment in the graphite grade, the system is expected to produce predominantly hydrophilic heteroflocs. While this prevents recovery of graphite in the froth, the decreased LCO entrainment positively impacts graphite grade. It is also likely that the unaffected graphite is kinetically favored for its extraction in the froth.

Flocculation of black mass is recognized to be a complex phenomenon, and increasing the selectivity of the process requires carefully mapping out the behavior of multiple variables. In this paper, the complexity of the studied system was minimized by applying selective flocculation to a two-component system, consisting of analytically pure LCO and graphite, and with a minimum addition of flotation reagents (only a frother). For the process to be studied in conditions more akin to an industrial setting, research must be conducted with model black mass samples that include multiple cathode chemistries. Pulp conditions would need to be tailored to enable the flocculation of multiple cathodes, while preventing the flocculation of graphite.

In addition, it will be necessary to study the flocculation process with industrial black mass waste, in which residual battery components are expected to be present. Binder polymers, electrolytes, and current collectors are expected to form multiple distinctive interfaces in the studied system [57], and the possible adsorption of a flocculant on these non-target interfaces should be thoroughly understood. Furthermore, chemically selective flocculants should be studied and developed, as they could provide improved selectivity compared to electrically selective flocculants, especially in systems involving multiple components [30]. The chemical similarity of Li-ion battery cathode materials holds the promise that a flocculant could be made chemically selective towards multiple cathodes. The mechanical parameters during flocculant/dispersant conditioning, such as the energy of mixing and conditioning time, would also be necessary to study, as floc formation and growth have been reported to be affected by said parameters [47]. The interaction of the flotation chemicals and the dispersing/flocculating agents should also be studied.

Finally, selective flocculation might be attractive in the context of cathode chemistries produced from low-cost metals. LiFePO<sub>4</sub> (LFP) for example, is a cathode chemistry that has become popular in the recent years, and recycling it via chemical methods is widely considered uneconomical. Furthermore, the particle size of LFP has been reported to be

noticeably finer compared to LCO or NMC [58]. In the near future, direct recycling might be the only option for the economic recycling of LFP waste. For this reason, studying selective flocculation processes for LFP black mass might be beneficial.

## 5. Conclusions

In addition to liberation requirements for the efficient recycling of battery materials, mechanical entrainment of ultrafine cathode particles remains an impending challenge. Indeed, the control of particle sizes is necessary to recover the graphite at >99% purity, even if the black mass is fully liberated. Selective flocculation was studied for such particle size modification in the present study, and it is deemed a promising approach to improve the recycling rate of spent LIBs, and to achieve circularity for battery-grade graphite, which has been largely neglected in current industrial recycling schemes.

The conclusions from the research work hereby presented can be summarized as follows:

- Froth flotation can be applied for recovering high-quality graphite from LIB waste, provided the black mass is fully liberated and the cathode particle size is optimized to prevent entrainment. In the absence of ultrafine cathode particles (ideal case), a graphite concentrate grade of 99.4% was achieved with 54.7% recovery, in single-stage flotation.
- When ultrafine cathode particles < 10 µm were included in the model black mass feed (realistic case), a graphite concentrate grade of 98.2% was achieved with a recovery of 71.3%. This result suggests that cathode entrainment needs to be prevented for battery-grade graphite to be recovered in single-stage flotation.
- Laser diffraction particle size measurements revealed that, when 10<sup>-5</sup> M HCl (aq.) was applied as a medium of flocculation, single-mineral dispersions of LCO would flocculate efficiently when a cationic polyacrylamide flocculant was used. Under similar conditions, single-mineral dispersions of graphite were not affected by any of the studied flocculants.
- The selectivity of flocculation in a mixed-mineral system was studied by performing flotation experiments with flocculated model black mass (realistic case), under a similar dispersive medium as in single-mineral particle size measurements. A graphite concentrate of 98.4% grade was observed with the flocculated feed, associated with a recovery of 40.5%. With the addition of a dispersant (0.5 wt.-% SHMP), graphite recovery from the flocculated feed could be increased to 52.5%, while maintaining a 98.4% grade. The results suggest that particle size control via selective flocculation is a viable method for cathode entrainment prevention in black mass flotation, and that SHMP is a potential dispersant for preventing graphite from heteroflocculating.
- It was observed that the flocculant type needs to be carefully considered to improve the selectivity of flocculation in mixed-mineral systems. Branched polymer variants appeared to provide improved selectivity over linear variants. Moreover, overdosage of the flocculant needs to be avoided. The data in this experimental series suggest that a concentration of 20 g/t is optimal for the selectivity of the flocculation process with SNF FO 4498 and SNF FO 5449 flocculants.

**Author Contributions:** Conceptualization, R.S.-G.; methodology, T.R., N.A.-G. and R.S.-G.; software, T.R. and N.A.-G.; validation, T.R., N.A.-G. and R.S.-G.; formal analysis, T.R.; investigation, T.R. and N.A.-G.; resources, R.S.-G.; data curation, T.R.; writing—original draft preparation, T.R. and N.A.-G.; writing—review and editing, R.S.-G.; visualization, T.R. and N.A.-G.; supervision, R.S.-G.; project administration, R.S.-G.; funding acquisition, R.S.-G. All authors have read and agreed to the published version of the manuscript.

**Funding:** This research was funded by the Business Finland BATCircle2.0 project, grant number 44886/31/2020.

**Data Availability Statement:** The authors confirm that the data supporting the findings of this study are available within the article.

**Acknowledgments:** T.R. thanks the Technology Industries of Finland Centennial Foundation (Steel and Metal Producers Fund) for a Doctoral studies scholarship.

**Conflicts of Interest:** The authors declare no conflict of interest.

## Appendix A

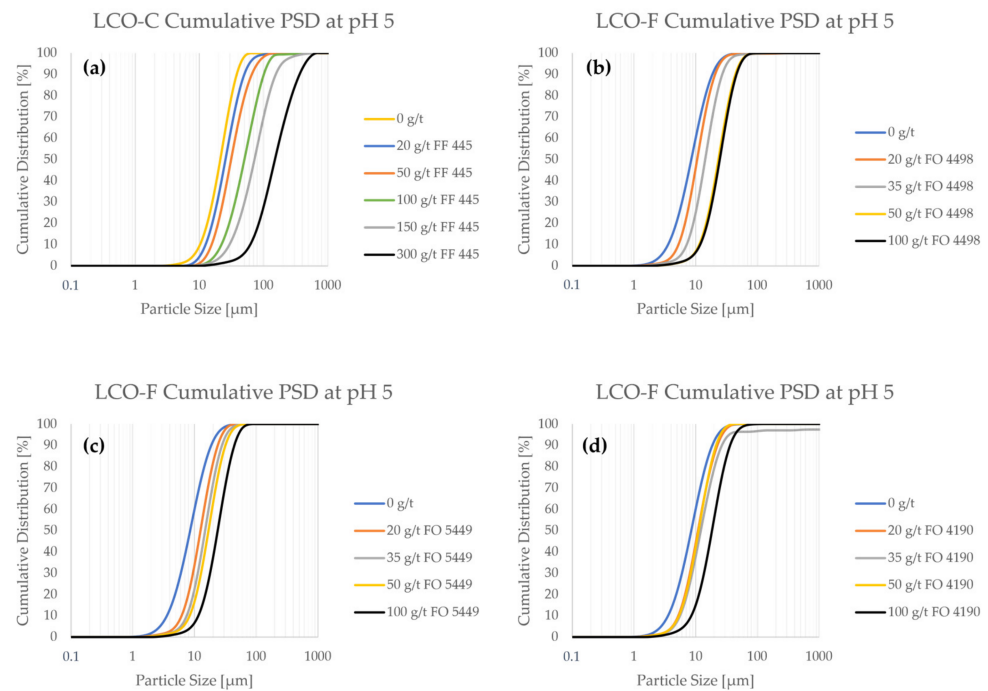


**Figure A1.** The cumulative particle size distributions as a function of flocculant concentration in pH 5.

## References

- Velázquez-Martínez, O.; Valio, J.; Santasalo-Aarnio, A.; Reuter, M.; Serna-Guerrero, R. A critical review of lithium-ion battery recycling processes from a circular economy perspective. *Batteries* **2019**, *5*, 68. [CrossRef]
- Le Varlet, T.; Schmidt, O.; Gambhir, A.; Few, S.; Staffell, I. Comparative life cycle assessment of lithium-ion battery chemistries for residential storage. *J. Energy Storage* **2020**, *28*, 101230. [CrossRef]
- Nitta, N.; Wu, F.; Lee, J.T.; Yushin, G. Li-ion battery materials: Present and future. *Mater. Today* **2015**, *18*, 252–264. [CrossRef]
- Ali, H.; Khan, H.A.; Pecht, M.G. Circular economy of Li Batteries: Technologies and trends. *J. Energy Storage* **2021**, *40*, 102690. [CrossRef]
- Harper, G.; Sommerville, R.; Kendrick, E.; Driscoll, L.; Slater, P.; Stolkin, R.; Walton, A.; Christensen, P.; Heidrich, O.; Lambert, S.; et al. Recycling lithium-ion batteries from electric vehicles. *Nature* **2019**, *575*, 75–86. [CrossRef] [PubMed]
- European Commission. Proposal for a Regulation of the European Parliament and of the Council Concerning Batteries and Waste Batteries, Repealing Directive 2006/66/EC and Amending Regulation (EU) No 2019/1020. Available online: <https://eur-lex.europa.eu/legal-content/EN/TXT/?uri=CELEX%3A52020PC0798> (accessed on 2 December 2022).
- European Commission. Study on the EU's List of Critical Raw Materials; European Commission: 2020. Available online: <https://rmis.jrc.ec.europa.eu/?page=crm-list-2020-e294f6> (accessed on 2 December 2022).
- Liu, J.; Shi, H.; Hu, X.; Geng, Y.; Yang, L.; Shao, P.; Luo, X. Critical strategies for recycling process of graphite from spent lithium-ion batteries: A review. *Sci. Total Environ.* **2022**, *816*, 151621. [CrossRef]
- Vanderbruggen, A.; Hayagan, N.; Bachmann, K.; Ferreira, A.; Werner, D.; Horn, D.; Peuker, U.; Serna-Guerrero, R.; Rudolph, M. Lithium-Ion Battery Recycling—Influence of Recycling Processes on Component Liberation and Flotation Separation Efficiency. *ACS EST Eng.* **2022**, *2*, 2130–2141. [CrossRef]
- Traore, N.; Kelebek, S. Characteristics of Spent Lithium Ion Batteries and Their Recycling Potential Using Flotation Separation: A Review. *Miner. Process. Extr. Metall. Rev.* **2022**, 1–29. [CrossRef]
- Huang, Y.; Han, G.; Liu, J.; Chai, W.; Wang, W.; Yang, S.; Su, S. A stepwise recovery of metals from hybrid cathodes of spent Li-ion batteries with leaching-flotation-precipitation process. *J. Power Sources* **2016**, *325*, 555–564. [CrossRef]
- He, Y.; Zhang, T.; Wang, F.; Zhang, G.; Zhang, W.; Wang, J. Recovery of LiCoO<sub>2</sub> and graphite from spent lithium-ion batteries by Fenton reagent-assisted flotation. *J. Clean. Prod.* **2017**, *143*, 319–325. [CrossRef]
- Yu, J.; He, Y.; Ge, Z.; Li, H.; Xie, W.; Wang, S. A promising physical method for recovery of LiCoO<sub>2</sub> and graphite from spent lithium-ion batteries: Grinding flotation. *Sep. Purif. Technol.* **2018**, *190*, 45–52. [CrossRef]

14. Liu, J.; Wang, H.; Hu, T.; Bai, X.; Wang, S.; Xie, W.; Hao, J.; He, Y. Recovery of LiCoO<sub>2</sub> and graphite from spent lithium-ion batteries by cryogenic grinding and froth flotation. *Miner. Eng.* **2020**, *148*, 106223. [[CrossRef](#)]
15. Ruismäki, R.; Rinne, T.; Dańczak, A.; Taskinen, P.; Serna Guerrero, R.; Jokilaakso, A. Integrating flotation and pyrometallurgy for recovering graphite and valuable metals from battery scrap. *Metals* **2020**, *10*, 680. [[CrossRef](#)]
16. Folleyan, T.O.; Lipson, A.L.; Durham, J.L.; Pinegar, H.; Liu, D.; Pan, L. Direct Recycling of Blended Cathode Materials by Froth Flotation. *Energy Technol.* **2021**, *9*, 2100468. [[CrossRef](#)]
17. Vanderbruggen, A.; Sygusch, J.; Rudolph, M.; Serna-Guerrero, R. A contribution to understanding the flotation behavior of lithium metal oxides and spheroidized graphite for lithium-ion battery recycling. *Colloids Surf. A Physicochem. Eng. Asp.* **2021**, *626*, 127111. [[CrossRef](#)]
18. Vanderbruggen, A.; Salces, A.; Ferreira, A.; Rudolph, M.; Serna-Guerrero, R. Improving Separation Efficiency in End-of-Life Lithium-Ion Batteries Flotation Using Attrition Pre-Treatment. *Minerals* **2022**, *12*, 72. [[CrossRef](#)]
19. Rinne, T.; Klemettinen, A.; Klemettinen, L.; Ruismäki, R.; O'Brien, H.; Jokilaakso, A.; Serna-Guerrero, R. Recovering value from end-of-life batteries by integrating froth flotation and pyrometallurgical copper-slag cleaning. *Metals* **2021**, *12*, 15. [[CrossRef](#)]
20. Dańczak, A.; Ruismäki, R.; Rinne, T.; Klemettinen, L.; O'Brien, H.; Taskinen, P.; Jokilaakso, A.; Serna-Guerrero, R. Worth from Waste: Utilizing a Graphite-Rich Fraction from Spent Lithium-Ion Batteries as Alternative Reductant in Nickel Slag Cleaning. *Minerals* **2021**, *11*, 784. [[CrossRef](#)]
21. Salces, A.M.; Bremerstein, I.; Rudolph, M.; Vanderbruggen, A. Joint recovery of graphite and lithium metal oxides from spent lithium-ion batteries using froth flotation and investigation on process water re-use. *Miner. Eng.* **2022**, *184*, 107670. [[CrossRef](#)]
22. Saneie, R.; Abdollahi, H.; Ghassa, S.; Azizi, D.; Chehreh Chelgani, S. Recovery of Copper and Aluminum from Spent Lithium-Ion Batteries by Froth Flotation: A Sustainable Approach. *J. Sustain. Metall.* **2022**, *8*, 386–397. [[CrossRef](#)]
23. Cheng, Q.; Marchetti, B.; Chen, X.; Xu, S.; Zhou, X.D. Separation, Purification, Regeneration and Utilization of Graphite Recovered from Spent Lithium-Ion Batteries—A Review. *J. Environ. Chem. Eng.* **2022**, *10*, 107312. [[CrossRef](#)]
24. Fuerstenau, M.C.; Han, K.N. *Principles of Mineral Processing*; SME: Englewood, CO, USA, 2003.
25. Gupta, A.; Yan, D.S. *Mineral Processing Design and Operation: An Introduction*; Elsevier: Amsterdam, The Netherlands, 2006.
26. Vanderbruggen, A.; Gugala, E.; Blannin, R.; Bachmann, K.; Serna-Guerrero, R.; Rudolph, M. Automated mineralogy as a novel approach for the compositional and textural characterization of spent lithium-ion batteries. *Miner. Eng.* **2021**, *169*, 106924. [[CrossRef](#)]
27. Farrokhpay, S.; Filippov, L.; Fornasiero, D. Flotation of Fine Particles: A Review. *Miner. Process. Extr. Metall. Rev.* **2021**, *42*, 473–483. [[CrossRef](#)]
28. Wang, C.; Wang, P.; Tan, X.; Huang, G.; Kou, J.; Sun, C.; Liu, Q. Selective aggregation of fine quartz by polyaluminum chloride to mitigate its entrainment during fine and ultrafine mineral flotation. *Sep. Purif. Technol.* **2021**, *279*, 119606. [[CrossRef](#)]
29. Wang, C.; Sun, C.; Liu, Q. Entrainment of Gangue Minerals in Froth Flotation: Mechanisms, Models, Controlling Factors, and Abatement Techniques—A Review. *Min. Metall. Explor.* **2021**, *38*, 673–692. [[CrossRef](#)]
30. Mathur, S.; Singh, P.; Moudgil, B.M. Advances in selective flocculation technology for solid-solid separations. *Int. J. Miner. Process.* **2000**, *15*, 201–222. [[CrossRef](#)]
31. Wang, D.; Liu, Q. Influence of aggregation/dispersion state of hydrophilic particles on their entrainment in fine mineral particle flotation. *Miner. Eng.* **2021**, *166*, 106835. [[CrossRef](#)]
32. Panda, L.; Banerjee, P.K.; Biswal, S.K.; Venugopal, R.; Mandre, N.R. Performance evaluation for selectivity of the flocculant on hematite in selective flocculation. *Int. J. Miner. Metall. Mater.* **2013**, *20*, 1123–1129. [[CrossRef](#)]
33. Panda, L.; Banerjee, P.K.; Biswal, S.K.; Venugopal, R.; Mandre, N.R. Modelling and optimization of process parameters for beneficiation of ultrafine chromite particles by selective flocculation. *Sep. Purif. Technol.* **2014**, *132*, 666–673. [[CrossRef](#)]
34. Panda, L.; Venugopal, R.; Mandre, N.R.; Singh, V.; Banerjee, P.K. Assessment and Mechanism Investigation of Selective Flocculation Process for Ultrafine Chromite Particle. *Sep. Sci. Technol.* **2015**, *50*, 1050–1058. [[CrossRef](#)]
35. Dogu, I.; Arol, A.I. Separation of dark-colored minerals from feldspar by selective flocculation using starch. *Powder Technol.* **2004**, *139*, 258–263. [[CrossRef](#)]
36. Cheng, K.; Wu, X.; Tang, H.; Zeng, Y. The flotation of fine hematite by selective flocculation using sodium polyacrylate. *Miner. Eng.* **2022**, *176*, 107273. [[CrossRef](#)]
37. Hao, H.; Li, L.; Somasundaran, P.; Yuan, Z. Adsorption of pregelatinized starch for selective flocculation and flotation of fine siderite. *Langmuir* **2019**, *35*, 6878–6887. [[CrossRef](#)]
38. Lima, R.M.F.; Abreu, F.D.P.V.F. Characterization and concentration by selective flocculation/magnetic separation of iron ore slimes from a dam of Quadrilátero Ferrífero—Brazil. *J. Mater. Res. Technol.* **2020**, *9*, 2021–2027. [[CrossRef](#)]
39. Wang, Z.; Liu, N.; Zou, D. Interface adsorption mechanism of the improved flotation of fine pyrite by hydrophobic flocculation. *Sep. Purif. Technol.* **2021**, *275*, 119245. [[CrossRef](#)]
40. Zhang, J.; Yang, C.; Niu, F.; Gao, S. Molecular dynamics study on selective flotation of hematite with sodium oleate collector and starch-acrylamide flocculant. *Appl. Surf. Sci.* **2022**, *592*, 153208. [[CrossRef](#)]
41. Loganathan, S.; Sankaran, S. Surface chemical and selective flocculation studies on iron oxide and silica suspensions in the presence of xanthan gum. *Miner. Eng.* **2021**, *160*, 106668. [[CrossRef](#)]
42. Ding, K.; Laskowski, J. Effect of conditioning on selective flocculation with polyacrylamide in the coal reverse flotation. *Miner. Process. Extr. Metall.* **2007**, *116*, 108–114. [[CrossRef](#)]

43. Liang, L.; Tan, J.; Li, Z.; Peng, Y.; Xie, G. Coal flotation improvement through hydrophobic flocculation induced by polyethylene oxide. *Int. J. Coal Prep. Util.* **2016**, *36*, 139–150. [[CrossRef](#)]
44. Zou, W.; Gong, L.; Huang, J.; Zhang, Z.; Sun, C.; Zeng, H. Adsorption of hydrophobically modified polyacrylamide P (AM-NaAA-C16DMAAC) on model coal and clay surfaces and the effect on selective flocculation of fine coal. *Miner. Eng.* **2019**, *142*, 105887. [[CrossRef](#)]
45. Yu, B.; Che, X.; Zheng, Q. Flotation of ultra-fine rare-earth minerals with selective flocculant PDHA. *Miner. Eng.* **2014**, *60*, 23–25. [[CrossRef](#)]
46. Yu, M.; Mei, G.; Li, Y.; Liu, D.; Peng, Y. Recovering rare earths from waste phosphors using froth flotation and selective flocculation. *Miner. Metall. Process.* **2017**, *34*, 161–169. [[CrossRef](#)]
47. Attia, Y.A. Development of a selective flocculation process for a complex copper ore. *Int. J. Miner. Process.* **1977**, *4*, 209–225. [[CrossRef](#)]
48. Somasundaran, P.; Das, K.K.; Yu, X. Selective flocculation. *Curr. Opin. Colloid Interface Sci.* **1996**, *1*, 530–534. [[CrossRef](#)]
49. Somasundaran, P.; Runkana, V. Selective Flocculation of Fines. *Trans. Nonferrous Met. Soc.* **2000**, *10*, 8–11.
50. Owen, A.T.; Fawell, P.D.; Swift, J.D.; Farrow, J.B. The impact of polyacrylamide flocculant solution age on flocculation performance. *Int. J. Miner. Process.* **2002**, *67*, 123–144. [[CrossRef](#)]
51. Van de Ven, T.G.M.; Alinec, B. Heteroflocculation by asymmetric polymer bridging. *J. Colloid Interface Sci.* **1996**, *181*, 73–78. [[CrossRef](#)]
52. Liang, L.; Zhang, T.; Peng, Y.; Xie, G. Inhibiting heterocoagulation between microcrystalline graphite and quartz by pH modification and sodium hexametaphosphate. *Colloids Surf. A Physicochem. Eng. Asp.* **2018**, *553*, 149–154. [[CrossRef](#)]
53. Fuerstenau, D.W. Zeta potentials in the flotation of oxide and silicate minerals. *Adv. Colloid Interface Sci.* **2005**, *114*, 9–26. [[CrossRef](#)] [[PubMed](#)]
54. Zhang, G.; He, Y.; Wang, H.; Feng, Y.; Xie, W.; Zhu, X. Removal of organics by pyrolysis for enhancing liberation and flotation behavior of electrode materials derived from spent lithium-ion batteries. *ACS Sustain. Chem. Eng.* **2020**, *8*, 2205–2214. [[CrossRef](#)]
55. Zhang, G.; Ding, L.; Yuan, X.; He, Y.; Wang, H.; He, J. Recycling of electrode materials from spent lithium-ion battery by pyrolysis-assisted flotation. *J. Environ. Chem. Eng.* **2021**, *9*, 106777. [[CrossRef](#)]
56. Attia, Y.A. Fine particle separation by selective flocculation. *Sep. Sci. Technol.* **1982**, *17*, 485–493. [[CrossRef](#)]
57. Zhang, W.; Wang, D.; Zheng, W.T. A semiconductor-electrochemistry model for design of high-rate Li ion battery. *J. Energy Chem.* **2020**, *41*, 100–106. [[CrossRef](#)]
58. Jiang, X.T.; Wang, P.; Li, L.H.; Yu, J.; Yin, Y.X.; Hou, F. Recycling process for spent cathode materials of LiFePO<sub>4</sub> batteries. *Mater. Sci. Forum* **2019**, *943*, 141–148. [[CrossRef](#)]

**Disclaimer/Publisher’s Note:** The statements, opinions and data contained in all publications are solely those of the individual author(s) and contributor(s) and not of MDPI and/or the editor(s). MDPI and/or the editor(s) disclaim responsibility for any injury to people or property resulting from any ideas, methods, instructions or products referred to in the content.